Properties and environments of [Ultra] Luminous Infrared Galaxy candidates around the south ecliptic pole

Małgorzata Bankowicz[1], Aleksander Herzig[1], Agnieszka Pollo[1,2], Katarzyna Małek[2] and ADF-S Team

1. Astronomical Observatory of the Jagiellonian University, Orla 171, 30–244 Kraków, Poland
2. National Centre for Nuclear Research, A. Sołtana 7, 05–400 Otwock, Poland

[Ultra] Luminous Infrared Galaxies ([U]LIRGs) are a rare class of galaxies whose exact mechanisms of activity and very high dust luminosity are still under debate, with the mixed role of galaxy mergers, starburst and AGN to be clarified. For 39 [U]LIRGs discovered in the AKARI Deep Field-South we attempted to evaluate galactic density in their vicinity based on the Digital Sky Survey (DSS) data and dedicated follow-up observations by the SAAO telescopes. We concluded that ULIRGs prefer environments with high but not extreme density while LIRGs are more often found also in denser environments. It may imply that ULIRGs appear most often in the environment of the cluster outskirts, where galaxy mergers are the most probable, and it supports the hypothesis that mergers play the crucial role in their activation.

1 Introduction

Luminous and Ultra Luminous InfraRed Galaxies (LIRGs and ULIRGs) are objects with total absolute infrared (IR) luminosities much higher than that of average galaxies ($L_{\rm dust} > 10^{11}\,{\rm L}_\odot$ and $L_{\rm dust} > 10^{12}\,{\rm L}_\odot$ for LIRGs and ULIRGs, respectively). They were first discovered by IRAS in late 1980s (Soifer et al., 1986). These objects are much more commonly found at higher redshifts (Symeonidis et al., 2013), but they are also seen in the local Universe (Kim & Sanders, 1998), though not so commonly. Extreme infrared luminosities of these sources are attributed mainly to their intensive star formation (Noeske et al., 2007; da Cunha et al., 2015), with a possible contribution from an active galactic nucleus (AGN).

Despite being very luminous in infrared, which is due to the significant dust component, they are moderately luminous in optical bands. This phenomenon can be explained by their very high star formation rates which are of the order of $\sim 100\,{\rm M}_\odot\,{\rm yr}^{-1}$. As an AGN contribution to the infrared luminosity of [U]LIRGs, albeit significant, is not that high, a major contributor to their emission remains star formation.

[U]LIRGs are often found in merging or interacting systems, at least at low redshifts, and therefore mergers are supposed to be a trigger of their activity (Veilleux et al., 2002). On high redshifts the situation is less clear: galaxies identified as ULIRGs often look like normal galaxies, not in a merger state. As a result, there is no consensus in the literature yet what is the exact mechanism of the extreme activity of [U]LIRGs. It needs to be ascertained whether a merger is a trigger for both an AGN and star formation, which then develop independently or there might

exist a link between them. If indeed there is a connection it needs to be researched whether, for instance, it is an AGN which triggers or stimulates the star formation (Veilleux et al., 2009). It is not known either if mergers are necessary to trigger an [U]LIRG or an activation of an AGN without a merger can play this role.

If the hypothesis assuming the key role of galactic mergers in the origin of ULIRGs is correct, they should be more often found in environments in which mergers are most likely to happen. Simulations demonstrate that mergers should be most probable in medium to high, but not extreme, density environments (Lin et al., 2010). In this paper we address this problem making use of the sample of ULIRGs identified by Małek et al. (2014).

2 Data and methodology

We used data from Akari Deep Field - South (ADF-S) survey. ADF-S covers an area of $12.6\,\mathrm{deg}^2$, centered at $\alpha = 4^\mathrm{h}44^\mathrm{m}00^\mathrm{s}$ and $\delta = -53°20'00''$ and it has been observed in four AKARI far-infrared (FIR) filters centered at 65 μm, 90 μm, 140 μm, and 160 μm, which resulted in a catalog of more than 2,000 sources detected at 90 μm down to 20 mJy (Shirahata et al., 2009). Małek et al. (2010) cross-correlated ADF-S sources detected at 90 μm and brighter than 30.1 mJy with public databases (SIMBAD, NED, IRSA) and created a multi-wavelength catalog of 545 objects with optical counterparts. For 183 of them, also spectroscopic data were found, which then were used by Małek et al. (2014) to calibrate high quality photometric redshifts of the 113 further objects, estimated with the aid of the CIGALE code (Noll et al., 2009; Serra et al., 2011).

For the purposes of the analysis presented here, the sample was further reduced to the redshift range of $z \geq 0.05$ (as the estimation of photometric redshifts below this value is not very secure) and a sample of galaxies with the best covered spectral energy distributions (SEDs) and (by the definision of the ADF-S sample) with at least one measurement in the FIR. For 27 galaxies Herschel/SPIRE measurements were included into calculations. Subsequently, in Małek et al. (2017), we estimated physical properties of 69 galaxies from this catalog with the most reliable data, based on SED fitting performed with the aid of the CIGALE code. To take into account all possible sources of emission, the model by Fritz et al. (2006) for the AGN contribution, the model by Calzetti et al. (2000) for the dust attenuation, the double decreasing exponential star-formation history, the stellar population synthesis models of Maraston (2005) and two dust emission models by Casey (2012) and by Dale et al. (2014) were applied to construct the fitted SEDs.

Subsequently, for each galaxy from our sample, we estimated local projected density of galaxies around it (based distance to nth neighbour; for review see e.g. Muldrew et al., 2012). For these measurements we made use of optical images from the Digital Sky Survey (DSS), which is a collection of scanned plates of older catalogs, as this is the only publicly available optical survey covering all the ADF-S field. The DSS coverage sufficient for our measurements is provided in two filters: B_j and R (based on APM Sky Catalogue photometry down to 22.5 and 21 mag respectively). We excluded stellar objects and calculated optical magnitudes of all galaxies (recalculating the B_j filter to the standard Johnson B filter) in the vicinity of our targets directly from the DSS plate scans using Source Extractor software. There were two reasons for that: (1) we wanted to be sure the photometry in all the fields

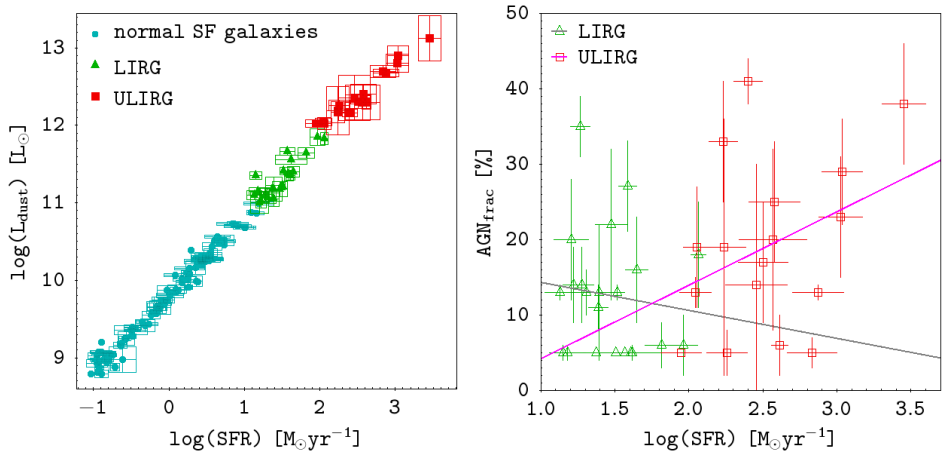

Fig. 1: Left panel: relation between dust luminosity $L_{\rm dust}$ and star formation rate (SFR) for our whole ADF-S sample. Right panel: relation between AGN fraction for ADF-S LIRGs and ULIRGs and SFR. Teal circles, green triangles and red squares denote normal SF galaxies, LIRGs and ULIRGs, respectively. On the right panel straight grey and pink lines represent best fitted linear relations between presented parameters for LIRGs and ULIRGs, respectively.

is performed in a uniform way (2) not all the objects of interest visible in the fields around our targets had previously estimated and publicly available magnitudes.

For better coverage in the optical regime more observational data are needed. We performed observations and acquired fluxes in $BVRI$ filters of our identified [U]LIRGs at the South African Astronomical Observatory, making use of the 1m and 2m telescopes at the SAAO. Data are being reduced now. These additional optical fluxes will allow to constrain better the optical (stellar) part of the fitted models. This will allow to obtain more accurate physical parameters of investigated galaxies, along with more precise astrometry providing better density estimations.

3 Results and conclusions

Based on the SED fitting we estimated physical properties (such as total dust luminosity, star formation rate, AGN fraction, stellar mass, dust mass and dust temperature) of our galaxy sample. Mean values of selected parameters: dust luminosity and mass, star formation rate (SFR) and AGN fraction are presented in Tab. 1. Based on these parameters in the ADF-S field we classified 22 LIRGs and 17 ULIRGs, spanning over in redshift range $0.06 \leq z \leq 1.23$. 63% among our ADF-S LIRGs and ULIRGs was found to have a significant contribution from AGN. However, there is a difference between these two classes: ULIRGs most commonly posses type 2 AGN (which corresponds to edge-on view of the torus) while LIRGs harbour both types of AGN (Małek et al., 2017).

Galaxies from our sample are rather massive with median value of stellar mass equal to $10^{9.38} \pm 10^{0.38}\,{\rm M}_{\odot}$. At the same time, they are actively SF with their mean SFR increasing stellar mass, with dust mass, and in particular with the luminosity of the dust, which is in agreement with the Kennicutt (1998) law, with average values

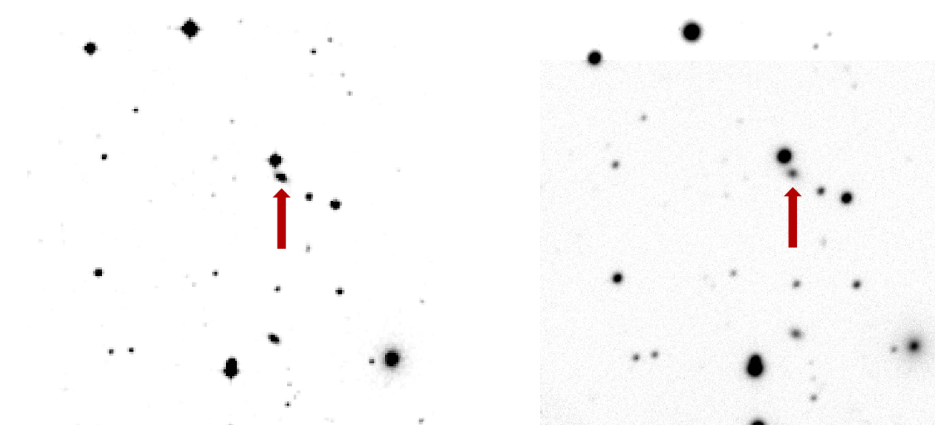

Fig. 2: Left panel: the DSS image of the field containing a source ADF-S 402. Right panel: our new SAAO observations from 1m telescope of this object and its neighbourhood. Red arrow indicates our target.

from $0.47 \pm 0.21\,\mathrm{M}_\odot\,\mathrm{yr}^{-1}$ for normal SFR galaxies, through $1.47 \pm 0.20\,\mathrm{M}_\odot\,\mathrm{yr}^{-1}$ for LIRGs up to $2.53 \pm 0.39\,\mathrm{M}_\odot\,\mathrm{yr}^{-1}$ for ULIRGs. This tight relation between SFR and L_{dust} is shown on the left panel of Fig. 1.

On the right panel of Fig. 1 we present $\mathrm{AGN}_{\mathrm{frac}}$ (fraction of energy from the AGN in the galaxy spectrum) vs. SFR relation for ADF-S LIRGs and ULIRGs. This plot demonstrates that in ULIRGs the AGN fraction increases with the increasing SFR, while for LIRGs there is practically no correlation between the two (or even the trend can be read as opposite, but not with a high statistical significance). We can interpret this as a demonstration that in ULIRGs AGN activity and star formation are physically related phenomena, which is not the case for LIRGs.

	$\log(L_{\mathrm{dust}})\,[\mathrm{L}_\odot]$	$\log(\mathrm{SFR})\,[\mathrm{M}_\odot\,\mathrm{yr}^{-1}]$	$\mathrm{AGN}_{\mathrm{frac}}\,[\%]$	$\log(M_{\mathrm{dust}})\,[\mathrm{M}_\odot]$
ULIRGs	12.40 ± 0.32	2.53 ± 0.39	19.12 ± 6.76	8.69 ± 0.02
LIRGs	11.31 ± 0.25	1.47 ± 0.20	12.54 ± 3.59	7.46 ± 0.07
Normal SF	10.35 ± 0.32	0.47 ± 0.21	12.82 ± 1.72	6.43 ± 0.05

Table 1: Main physical parameters for ULIRGs, LIRGs and normal star forming galaxies (with $L_{\mathrm{dust}} \leq 10^{11}\,\mathrm{L}_\odot$) from ADF-S galaxies estimated by CIGALE SED fitting.

As mentioned above, we performed additional optical observations by the SAAO 2m and 1m telescopes in $BVRI$ filters. The collected images are now under reduction. Fig. 2 presents a comparison of images in R filer obtained from the DSS and from our SAAO observations, of a neighbourhood of an object ADF-S 402, which was identified with a source 2MASX_J04314162-5336324, and classified as ULIRG by our analysis. These new data will be used to obtain both : SED better fits (and, consequently, estimated physical parameters) of our sources and as a base for better local density measurements.

Here, in Fig. 3 we present our preliminary measurements of the environmental dependence of properties of the ADF-S sources based on the DSS images. Left panel presents the relation between the local density around ADF-S galaxies and their dust masses. [U]LIRGs, as we already mentioned, tend to posses more dust

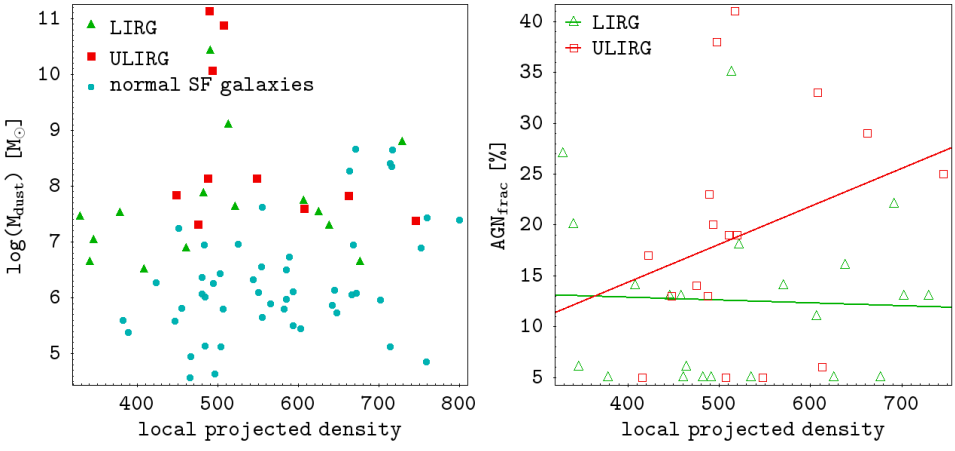

Fig. 3: Left panel: relation between dust mass and local projected density around ADF-S galaxies. Right panel: dependence of AGN fraction in ADF-S LIRGs and ULIRGs for ADF-S LIRGs and ULIRGs. Teal circles, green triangles and red squares denote normal SF galaxies, LIRGs and ULIRGs, respectively. At right panel straight lines denote linear regression: green for LIRGs and red for ULIRGs.

than normal SF galaxies. We can see that all ADF-S galaxies - SF galaxies, LIRGs and ULIRGs may be found in broad spectrum of environmental densities. However, ULIRGs tend to reside in medium density areas, and this preference is the strongest for the objects with the largest dust masses. This indicates that ULIRGs indeed tend to reside in areas of medium density, like outskirts of clusters, where mergers are more probable to occur. Right panel of Fig. 3 demonstrates that the AGN fraction for ULIRGs increases with environmental density, while for LIRGs – there is no correlation between the local density and AGN fraction. This result demonstrates, again, that there is a direct link between AGN activity of ULIRGs, its SF (as shown above) and its local environment (Bankowicz et al. in prep). LIRGs are much less prone to such environmental influence.

Acknowledgements. This research is based on observations with AKARI, a JAXA project with the participation of ESA. This research was supported by the Polish National Science Centre grant UMO-2016/23/N/ST9/01231.

References

Calzetti, D., et al., *ApJ* **533**, 682 (2000)

Casey, C. M., *MNRAS* **425**, 3094 (2012)

da Cunha, E., et al., *ApJ* **806**, 110 (2015)

Dale, D. A., et al., *ApJ* **784**, 83 (2014)

Fritz, J., Franceschini, A., Hatziminaoglou, E., *MNRAS* **366**, 767 (2006)

Kennicutt, R. C., Jr., *ARA&A* **36**, 189 (1998)

Kim, D.-C., Sanders, D. B., *ApJS* **119**, 41 (1998)

Lin, L., et al., *ApJ* **718**, 1158 (2010)

Małek, K., et al., *A&A* **514**, A11 (2010)
Małek, K., et al., *A&A* **562**, A15 (2014)
Małek, K., et al., *A&A* **598**, A1 (2017)
Maraston, C., *MNRAS* **362**, 799 (2005)
Muldrew, S. I., et al., *MNRAS* **419**, 2670 (2012)
Noeske, K. G., et al., *ApJL* **660**, L43 (2007)
Noll, S., Burgarella, D., Giovannoli, E., et al., *A&A* **507**, 1793 (2009)
Serra, P., Amblard, A., Temi, P., et al., *ApJ,* **740**, 22 (2011)
Shirahata, M., Matsuura, S., Hasegawa, S., et al., *PASJ* **61**, 737 (2009)
Soifer, B. T., et al., *ApJL* **303**, L41 (1986)
Symeonidis, M., et al., *MNRAS* **431**, 2317 (2013)
Veilleux, S., Kim, D.-C., Sanders, D. B., *ApJS* **143**, 315 (2002)
Veilleux, S., et al., *ApJS* **182**, 628 (2009)